On the Dynamics of Interacting Spreading Processes

by

Joshua Melander

B.S., Linfield College, 2013

_____

A THESIS

submitted in partial fulfillment of the
requirements for the degree

MASTER OF SCIENCE

Electrical & Computer Engineering
College of Engineering

KANSAS STATE UNIVERSITY
Manhattan, Kansas

2016

Approved by:

Major Professor
Faryad Darabi Sahneh

Copyright

Joshua Ryan Melander

2016

Abstract

A significant number of processes we observe in nature can be described as a spreading process; any agent which is compelled to survive by replicating through a population, examples include viruses, opinions, and information. Accordingly, a significant amount of thought power has been spent creating tools to aid in understanding spreading processes: How do they evolve? When do they thrive? What can we do to control them? Often times these questions are asked with respect to processes in isolation, when agents are free to spread to the maximum extent possible given topological and characteristic constraints. Naturally, we may be interested in considering the dynamics of multiple processes spreading through the same population, examples of which there are no shortage; we frequently characterize nature itself by the interaction and competition present at all scales of life. Recently the number of investigations into interacting processes, particularly in the context of complex networks, has increased. The roles of interaction among processes are varied from mutually beneficial to hostel, but the goals of these investigations has been to understand the role of topology in the ability of multiple processes to co-survive. A consistent feature of all present works — within the current authors knowledge — is that conclusions of coexistence are based on *marginal* descriptions population dynamics.

It is the main contribution of this work to explore the hypothesis that purely marginal population descriptions are insufficient indicators of co-survival between interacting processes. Specifically, evaluating coexistence based on non-zero marginal populations is an over-simplistic definition. We randomly generate network topologies via a community based algorithm, the parameters of which allow for trivially controlling possibility of coexistence. Both marginal *and* conditional probabilities of each process surviving is measured by stochastic simulations. We find that positive marginal probabilities for both processes existing long

term does not necessarily imply coexistence, and that marginal and conditional measurements only agree when layers are strongly anti-correlated (sufficiently distinct). In addition to the present thesis, this work is being prepared for a journal article publication.

The second portion of this thesis presents numerical simulations for the *Adaptive Contact - Susceptible Alert Infected Susceptible* model. The dynamics of interaction between an awareness process and an infectious process are computed over a multilayer network. The rate at which nodes "switch" their immediate neighbors (contacts) when exposed to the infection is varied and numerical solutions to the epidemic threshold are computed according to mean-field approximation. We find two unexpected cases where certain parameter configurations allow the epidemic threshold to either increase above or decrease below the theoretical limits of the layers when considered individually. These computations were performed as part of a separate journal article that has been accepted for publication.

Table of Contents

List of Figures

Acknowledgments

Thank you to my advisers Faryad Darabi Sahneh and Caterina Scoglio for their patience and mentoring over the past two years. Additional appreciation to the entire Electrical & Computer Engineering department; to the educators who helped to advance my knowledge, the students who welcomed me into the community, and to those wonderful people in the office who made every administrative experience as painless as possible. I am also grateful to the Computer & Information Science and Statistics departments for supplementing my learning with several interesting and useful courses. Finally, I would like to acknowledge National Science Foundation Award CIF-1423411.d for support while the conducting this work.

Chapter 1

Introduction

In this work we present investigations on the interactions between spreading processes. The case for studying interacting processes, where dynamics of multiple process mutually influence the evolution of each other, is not a difficult one to make due to their ubiquity in nature. Species competing for resources in their environment, two opposing viewpoints competing to spread through society, and infectious diseases spreading through human and animal populations are a few general examples of interacting processes that exist in everyday life. A significant portion of work on the dynamics of processes up to this point has considered processes spreading in isolation. Understanding how a single agent such as a virus, opinion, or piece of information, is compelled to survive by replicating through a population is continually impacting on how we interact with and design processes throughout society. However, our understanding is still limited in the sense that rarely do processes operate in a closed environment, the behavior we observe in the natural world arrises due to the interaction of *many* processes. The total output of these interactions is greater than the sum of each of their dynamics, processes interacting according to the most basic of principles can give rise to much richer behavior than a single process.

Modeling the dynamics of spreading processes over complex networks has proved an effective way to incorporate topology into the evolution of a process, it is thus a natural launching point for the additional consideration of the dynamics between multiple spreading

processes. Initial investigations have considered roles of interaction varying from processes that reinforce and aid in the spread of each other, to roles that are fundamentally opposed; though a majority focus specifically on competitive processes. One of the most fundamental characterizations of interacting processes is if and when co-survival is possible. Identifying thresholds for regions where coexistence occurs has been a primary focus in the most recent literature. By examining the link between contact structures and the thresholds of coexistence, researchers are aiming to illuminate how the topological conditions over which processes interact affect long term coexistence.

The approaches thus far used to model interacting processes on complex networks are straightforward extensions of those used to model isolated processes. Investigators posit a compartmental model of spreading dynamics and describe the evolution of the marginal population dynamics. For even the most simple models the exact solutions to these equations are intractable, thus a substantial amount of work has gone into providing useful approximations. *To the extent of the current author's knowledge, there are no exceptions in studies which use marginal descriptions of population dynamics to draw conclusions about the co-existence of processes.* As the main contribution of the present thesis, we put forth the hypothesis that:

1. *Marginal descriptions for population dynamics of interacting processes are not informative enough to characterize coexistence.*

We provide experimental support for this hypothesis by showing that the current working definition of coexistence based on purely marginal descriptions is at best inapplicable (situations when correctness is trivial) and at worst dead wrong. Argued further is that a coexistence definition based on conditional survival between processes is more appropriate.

We provide experimental support for this argument through stochastic simulations of competing processes on a community-based multilayer network (CBMN) model. The parameters of the CBMN allow for fine control over community structure. Providing sufficiently distinct communities enables coexistence through the creation of hubs where each process can thrive in relative isolation. At the end of simulations, the probability of each process

surviving is measured. A comparison between marginal and *conditional* measurements is presented.

The second portion of this thesis presents numerical simulations for the *Adaptive Contact - Susceptible Alert Infected Susceptible* model. The dynamics of interaction between an awareness process and an infectious process are computed over a multilayer network. The rate at which nodes "switch" their immediate neighbors (contacts) when exposed to the infection is varied and numerical solutions to the epidemic threshold are computed. We exibit two exceptional cases where certain parameter configurations allow the epidemic threshold to either increase above or decrease below the theoretical limits of the layers when considered individually.

1.1   Contributions

- Define the community-based multilayer network (CBMN) model for controlling the extent of community structure in random multilayer networks

- Provide experimental evidence for hypothesis 1, which states that marginal descriptions are insufficient characterizations of coexistence between interacting processes

- Present numerical calculations on the threshold behavior of competing awareness and infection processes with dynamic contact networks

Chapter 2

Background

2.1 Multilayer Networks

Complex networks are a powerful tool for understanding behaviors of large systems, though there are inherent limitations to considering only a single network. Extending the theory of complex networks to incorporate relationships between *multiple* networks is done in an effort to model more complicated situations. Work on combining multiple networks is new enough that a consensus of terminology has yet to be reached. Combining networks by considering multiple types of edges between the same set of nodes has been referred to as multilayer[1] and multiplex[2], while combing multiple networks of different elements is often referred to as interconnected networks[3]. A simple illustration of multilayer networks can be seen in Figure 2.1. The primary use of multilayer networks in this thesis is to provide a robust framework for mediating the interaction of multiple processes.

In the present work, a multilayer network, $\mathcal{G} = (V, E_1, E_2, ..., E_L)$, is referred to as a construction of L sets of edges connecting a single set of nodes, V. Single layer graphs, $G_l = (V, E_l)$, are represented by an adjacency matrix A_l where the value at index $a_{ij} \geq 0$ is the strength of connection from node i to node j. A value of zero indicates the absence of a connection between nodes.
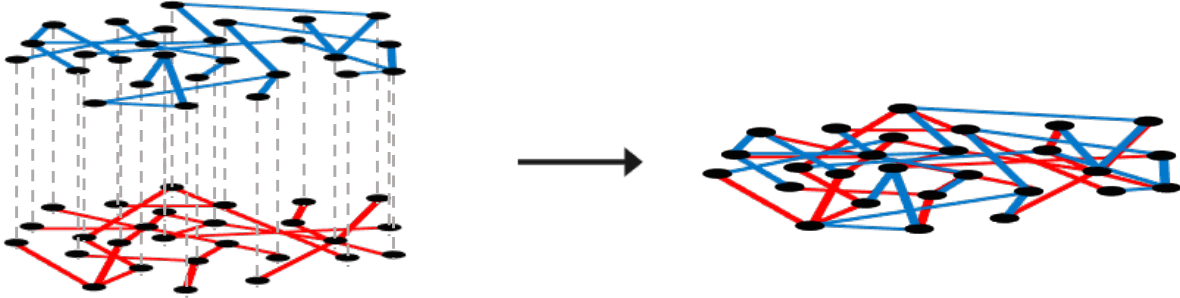
Figure 2.1: *Conceptual illustration of a multilayer network, a mathematical framework for incorporating multiple layers into a cohesive object*[4]

2.2 Spreading Processes

Compartmental models are used to model spreading dynamics over networks. In them, a set of states/compartments are defined which describe the state of each node at a given time. Rules of interactions are then by specifying by the transitions between states and the probability rates that govern them. The classic example of a compartmental spreading model is the *SIS* model which defines two compartments, *susceptible* and *infected*. Susceptible nodes may transition to the infected state depending on the per contact likelihood of transmission, β, multiplied by the number of infected neighbors. Nodes in the infected state will transition back to susceptible after an exponentially distributed amount time characterized by the rate δ.
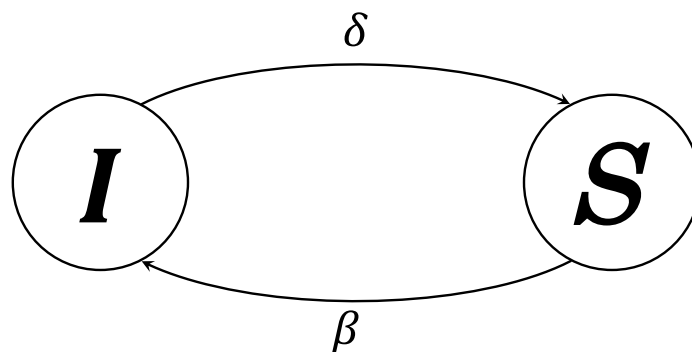
Figure 2.2: *State transition diagram for the susceptible, infected, susceptible model*

The sequence of states a given node i occupies forms a time series process, $x_i(t)$, where $x_i(t) = 0$ if susceptible at time t and $x_i(t) = 1$ if infected. The following Markov process

describes the probability of node i to transition to a different state at time $t + \Delta t$:

$$\Pr[x_i(t + \Delta t) = 1 | x_i(t) = 0, X(t)] = \beta I_i(t) \Delta t + o(\Delta t) \qquad (2.1)$$

$$\Pr[x_i(t + \Delta t) = 0 | x_i(t) = 1, X(t)] = \delta \Delta t + o(\Delta t) \qquad (2.2)$$

Where $I_i(t) = \sum_{j=1}^{N} a_{ij} x_j(t)$ is the number of infected neighbors of node i at time t and $X(t)$ is the overall state of the network. The rate of change of the expected value of $x_i(t)$ can be expressed as

$$\frac{d}{dt} E[x_i(t)] = \beta \sum_{j=1}^{N} a_{ij} E[x_j(t)] - \beta \sum_{j=1}^{N} a_{ij} E[x_i(t) x_j(t)] - \delta E[x_i(t)] \qquad (2.3)$$

The second, coupled, term of 2.3 presents an analytically and numerically intractable problem[3] and much work has gone into exploring the solutions to first-order approximations[5;6]. The approach to the SIS model seen here is very similar to those used in more complicated models, including those of interacting processes. After defining the states and transitions between them, marginal descriptions of state evolution similar to 2.1 and 2.2 are defined which include some terms relating the two.

2.3 Computational Tools - GEMFsim

The computational tasks of the present thesis fall into two categories: stochastic simulations and numerical calculations. Both are accomplished with the use of GEMFsim[7], which provides a general framework for computing the dynamics of compartmental models on complex networks. Tools provided by GEMFsim include stochastic simulations of spreading processes as well as numerical solutions to mean-field approximations. Compartmental models are specified by two classes of transitions, nodal and edge based. Edge based transitions are determined by the states of neighboring nodes which nodal transitions are not. Each class of transitions is represented by an $M \times M$ matrix, A_δ and A_β, where M is the number of model states. Values of transition matrices at index (i, j) are the probability parameter describing the transition from state i to j. To represent the SIS model described in 2.2 in GEMFsim, transition matrices would be defined as:

$$A_\delta = \begin{bmatrix} 0 & 0 \\ \delta & 0 \end{bmatrix} A_\beta = \begin{bmatrix} 0 & \beta \\ 0 & 0 \end{bmatrix} \tag{2.4}$$

Once a compartmental model is defined and a network specified, simulations are ran using an event based algorithim that samples from the Markov process described by the model. Two possible stop conditions may be specified to the simulation, either simulation length or number of events. One finished GEMFsim produces each node transition and the time at which it occurred.

Chapter 3

Coexistence of Interacting Processes

Regardless of the modality of interaction between processes, one of the most basic ways to characterize models of interacting processes is to evaluate the parameter space for regions in which it is possible for processes to coexist. The typical approach to answer this question is to examine the population of each process for an area where both are non-zero. At first glance this makes sense, but we argue in this chapter that is an over-simplification which conflates uncertainty in which process will dominate for coexistence. However, first we begin with studies that have previously investigated interacting processes through measures of coexistence.

3.1   Background

The first investigations of coexistence were performed on single layer networks, processes interacted and compete over the exact same contact topology. Newman et al.[8] were some of the first to account for topology in general by identifying thresholds for coexistence of two competitive spreading processes. In their approach, the first process spreads, immunizing nodes to the second process along the way. The spreading of the second process is then simulated over the remaining (residual) network. Coexistence is defined as the presence of large connected components in both the original and residual network, indicating both

processes may be sustained. In other words, if the first process leaves behind a network that is sufficiently large and connected to sustain the spread of a second process then the two are said to coexistence. Though the methodology neglects the actual interaction of processes dynamics, these results are some of the first to indicate the importance of distinct process contact networks in coexisting competitive processes.

Prakash et al.[9] also simulate competitive processes on a single layer network. Though process dynamics evolve together according to a generalized SIS model where nodes can be infected by either one virus or the other. The authors show that the stronger process will always and completely dominate the weaker process to extinction, regardless of topology. The authors of "Domination-time dynamics in susceptible-infected-susceptible virus competition on networks"[10] provide a deeper look into this idea by introducing a self-infection probability. Each node has a non-zero probability that it may spontaneously transition to one of the two process states, essentially making complete domination impossible. They show that even when one process is dominating, the self-infection probability can lead to a role reversal where the previously dominating processes is nearly completely minimized. The changing of regimes between which process dominates oscillates, continually switching between which process occupies a majority of the population. These findings indicate when all things are equal, the conditions that lead to domination can be tenuous, resulting from small statistical fluctuations that lead to runaway advantages.

The important conclusion of these investigations (at least in the context of the present work) is that the coexistence of competitive processes on a single layer is impossible[6;9–11]. This result is not all that surprising and is neatly summarized by the competitive exclusion principle of ecology which states that "complete competitors cannot coexist"[12]. If interacting processes are competing for the same resources (i.e. competing to occupy the same set nodes) over the *exact same set of relations* (i.e. edges) then the "ecosystem" of each process is the exact same and any competitive advantage, whether it be the result of stronger processes characteristics or chance benefit from some topological feature, will result in the complete domination by one process. Therefore a necessary condition for the long term coexistence of competing processes is sufficiently distinct contact networks.

One of the earliest investigations to take into account distinct network structures was published by Funk and Jansen[13], who refer to the concept of a multilayer network as an overlay network. In it the authors generalize Newman et al.[8] by specifying separate networks for each process and by varying the level of immunity granted by the first spreading process. They show that correlation between the node degree distributions of each topology is an important factor in whether or not both processes coexist. If degree distributions are positively correlated, then the first process is more effective at providing immunity to the second; implying that a *negative* correlation between node degree overlap correlates with coexistence. This idea has continually been affirmed by other studies of coexistence, which is that coexistence is enabled — at least in part — by the extent to which contact networks are distinct.[14–17].

A number of studies have aimed to identify thresholds between regions of coexistence and extinction in terms of process and topological characteristics of multilayer networks. Granell et al.[18] examine interacting processes in the context of an alert process competing with an infectious process on what the authors call a multiplex network, though it is the same as multilayer is defined in the present work. Using the microscopic Markov chain approach[6], authors identify a threshold for the suppression of the infection process as a function of the alertness process parameters. For the general case of competitive processes, in "Competitive epidemic spreading over arbitrary multilayer networks"[16] Sahneh et al. formalize the thresholds between regimes of coexistence in terms of the *survival threshold*, the point at which the probability becomes non-zero for a process to have a positve infection population. And the *absolute-dominance threshold* which denotes the point when one process drives the other to extinction. It logically follows that the survival threshold for one process is the absolute-dominance threshold of the other; the point at which one process completely dominates is the point at which the other is unable to survive. Thus coexistence is defined as the region that lies between the survival and complete-domination thresholds, as can be seen Figure 3.1.

Additional work by Wei et. al[19] model competing memes, also with the same extended SIS model used by several other studies by various authors[2;16;17;20]. Through spectral analy-
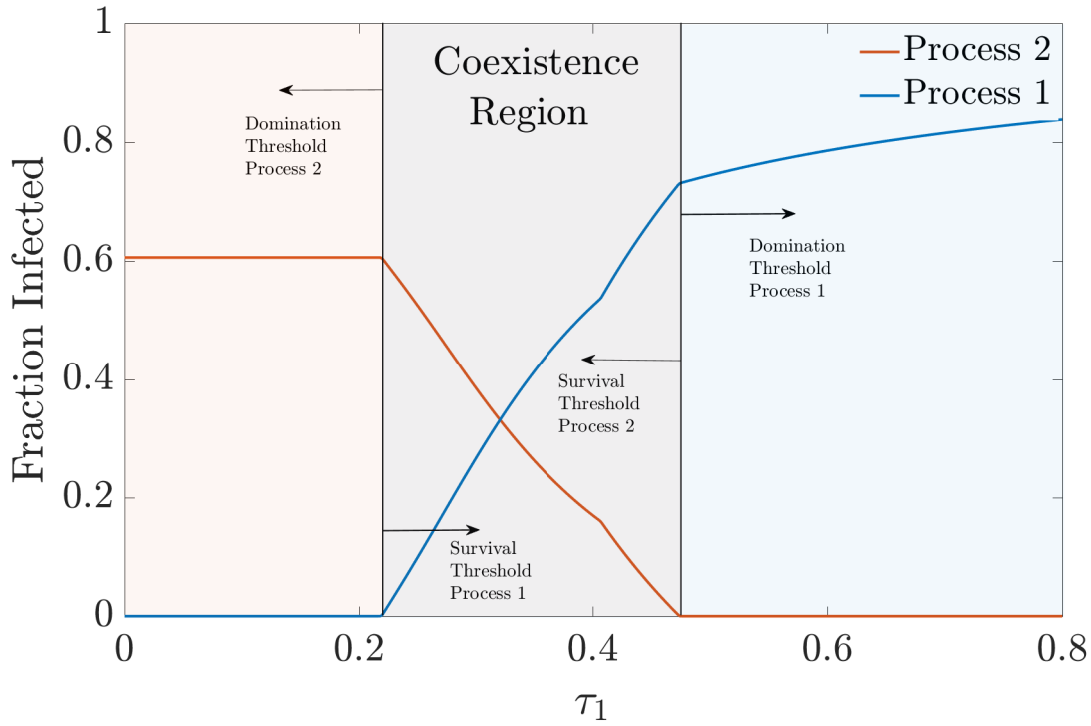
Figure 3.1: *This graph shows the survival and complete-domination thresholds for one of two competitive processes.*

sis of each layer the authors characterize coexistence between processes and develop a method for predicting which meme, i.e. process, will dominate the other to extinction. Interestingly, this approach is questioned by Sahneh et al[16] as being overly simplistic since, first, eigenvalues do not predict final outbreak size generally for all graphs, it is possible to construct a multilayer network such that the process corresponding to the layer with a smaller eigenvalue is able to dominate the other. Secondly, spectral methods are based on layer topology in isolation, there is no consideration of interaction dynamics. More recent work extends the same model to incorporate a full spectrum of interacting processes lying between competitive and cooperative[2;20] and provides framework "obtain formulas to accurately calculate epidemic thresholds of spreading processes that are impacted by other processes"[2]. Watkins et al.[17] extend the same model in a different direction by including heterogeneous epidemic parameters and showing how the the more robust parameter set can be used to optimize for the extinction of one of the processes.

A common theme of each study mentioned previously is that analyses rely on describing coexistence in terms of *marginal* probabilities. If the probability of each processes occupying a portion of the total population is non-zero, then they are said to coexist and the threshold is identified as the point when one process has a population of zero. The rest of this chapter presents experiments that demonstrate overlap between marginal survival rates does not necessarily indicate coexistence, since it may simply indicate an uncertainty in *which* process dominates.

3.1.1 The SI_1SI_2S Model

The SI_1SI_2S model is a straightforward extension of the classic SIS model. It describes the nodal dynamics of two competing processes, which are said to be competing because a node that is occupied by one process cannot be by the other. Thus processes compete to survive by occupying nodes which are acting as resources. As can be seen in Figure 3.2, nodes transition from the *susceptible* state to process 1 or process 2 based on transmission probabilities β_1 and β_2 respectively. Nodes in either *infected* state will transition back to *susceptible* automatically in a time decided by the exponential distributions characterized by δ_1 and δ_2. The infectivities of each process are defined as τ_1 and τ_2 which are each in turn equal to the ratio of process parameters:

$$
\begin{aligned}
\tau_1 &= \frac{\beta_1}{\delta_1} \\
\tau_2 &= \frac{\beta_2}{\delta_2}
\end{aligned}
\tag{3.1}
$$

3.2 Community Based Multilayer Network Model

Presently we develop a random network model with parameters that can be tuned to trivially induce coexistence. This is accomplished by defining a multilayer topology that provides (to varying degrees) a robust contact structure over a subset of the total population — referred to individually as *communities* — which supports the spreading of a single specific
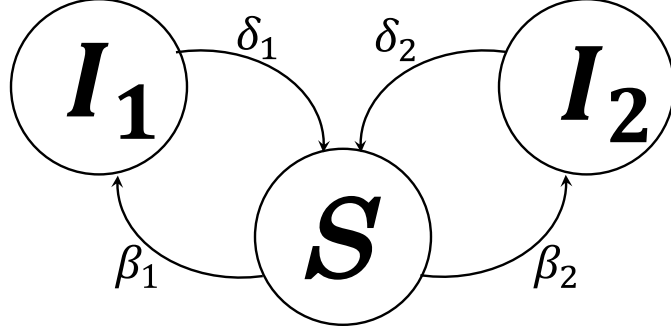
Figure 3.2: *State transition diagram for the SI_1SI_2S model*

process. The section of a network that is biased in favor a given process is referred to as the *home* community, the contact structure for a process in a community other than its own is inherently less connected.

In the case of two competing processes, the total population is split into two groups, **a** and **b**, where **a** is highly connected for one process and sparsely connected for the other and the reverse is true for community **b**. Consider then a multilayer network, $\mathcal{G} = (V, E_1, E_2)$ where V is the node set and E_1, E_2 are the edges connecting nodes in layer 1 and layer 2 respectively. The topology of each layer is randomly generated using the so called stochastic block model[21], which extends the classic Erydős-Róyni model to include community structure. Meaning that edges between members of the same community, as opposed to the entire network, are present given some probability threshold. Adjacency matrices for each community are labeled: C_{1a}, C_{1b}, C_{2a}, C_{2b}, and interconnections between them as W_1 & W_2. The composite adjacency matrices for each layer are expressed:

$$A_1 = \begin{bmatrix} C_{1a} & W_1 \\ W_1' & C_{1b} \end{bmatrix} \quad \& \quad A_2 = \begin{bmatrix} C_{2a} & W_2 \\ W_2' & C_{2b} \end{bmatrix} \tag{3.2}$$

Figure 3.2 shows an example topology for the CBMN. The probability threshold of each home community is multiplied by a factor $(1 + \epsilon)$, while thresholds for the away communities

remain at some constant p:

$$C_{1a,2b} = ER(N, p(1 + \epsilon))$$

$$C_{1b,2a} = ER(N, p)$$

(3.3)

Interconnection adjacency matrices, W_1 & W_2, define edges between nodes of different communities which are present based on a simple threshold probability p_c
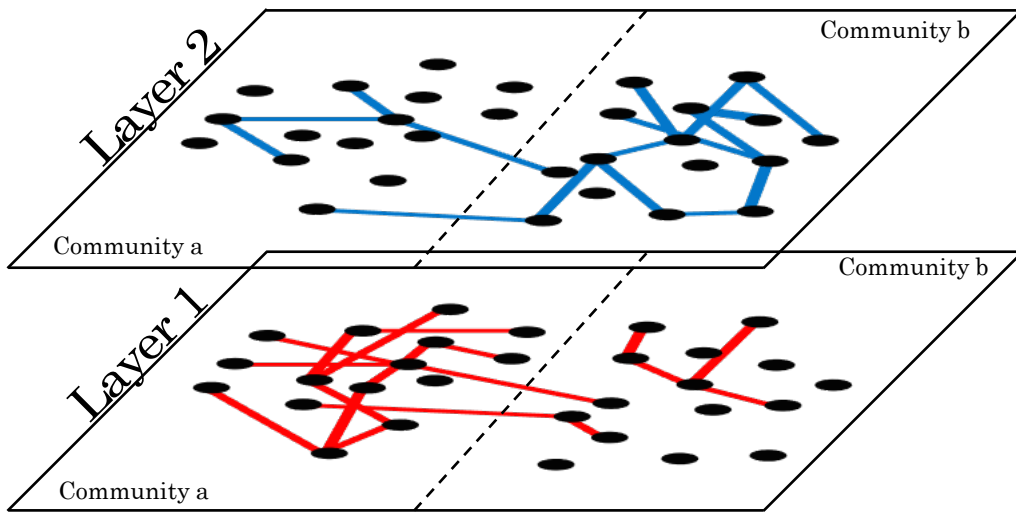
Figure 3.3: *Illustration of the community-based multilayer network model. Red lines in layer 1 describe contacts by which process 1 can be transmitted, blue lines in layer 2 describe the same for process 2. Note the higher level of connectivity in home communities, while contacts are more sparse in away communities. Edges that cross the center dotted lines are those are defined by W_1 & W_2.*

3.3 Measuring Coexistence

Crucial to the arguments of the current thesis is a closer examination of the definition of coexistence. We introduce the concept of survival to describe when a process has a steady state infection population greater than zero. Previous works typically have defined coexistence as the region when marginal population measures are positive for both process. The issue with this definition is that it includes the scenarios when domination by one

14

process is guaranteed, just not by which process. What is needed is a stricter definition of coexistence that depends on the *joint* probability of survival.

Consider two random variables, S_1 and S_2, which represent whether or not the corresponding process is present at the end of a simulation. Given that a process survives, the random variables take on the value 1, $s_1 = s_2 = 1$. Otherwise if extinct, $s_1 = s_2 = 0$. It follows then that there are four possible outcomes as can be seen in Figure 3.4

$$S_1$$

p_{00}	p_{10}
p_{01}	p_{11}
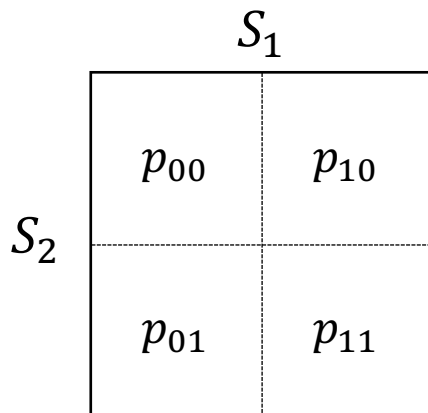
Figure 3.4: *Diagram of possible random variable outcomes for the two r.v S_1 and S_2. The first subscript digit represents the outcome of S_1 while the second represents S_2.*

The total outcome space forms a multinomial distribution. It follows then that the marginal distributions are binomial:

$$S_i \sim B(n, \mu_i) \tag{3.4}$$

The marginal survival probability is then simply equal to the mean of each binomial distribution:

$$\Pr(S_1 = 1) = \mu_1$$
$$\Pr(S_2 = 1) = \mu_2 \tag{3.5}$$

The typical working definition of coexistence is when both marginal probabilities of survival

are non-zero, i.e when both of the following expressions are true

$$\mu_1 > 0$$
$$\mu_2 > 0$$

(3.6)

We can express each of the likelihoods in 3.5 as the sum of two out of the four total outcomes (Figure 3.4), essentially integrating over both possible outcomes of the opposing process:

$$\Pr(S_1 = 1) = p_{10} + p_{11}$$
$$\Pr(S_2 = 1) = p_{01} + p_{11}$$

(3.7)

Note here that it is the second term of the preceding equations which technically captures coexistence, when *both* processes have survived. Due to the first terms however, it is possible for the conditions of 3.6 to be satisfied while the probability of both surviving is zero, $p_{11} = 0$.

Thus we posit that the definition of coexistence should be based on the probability of joint survival, specifically by conditioning survival probabilities on each other:

$$\Pr(S_1 = 1 | S_2 = 1) = \frac{p_{11}}{p_{01} + p_{11}}$$
$$\Pr(S_2 = 1 | S_1 = 1) = \frac{p_{11}}{p_{10} + p_{11}}$$

(3.8)

and define the threshold for coexistence as the point when either of the following expressions are true

$$\Pr(S_1 = 1 | S_2 = 1) > 0$$
$$\Pr(S_1 = 1 | S_2 = 1) > 0$$

(3.9)

or more simply, when $p_{11} > 0$

Although the difference between these two definitions of coexistence is subtle, we find that it is quite possible for large areas of a parameter space to lie in between the area of disagreement between the two definitions. These scenarios represent outcomes for which

16

domination is the only possibility though the specific process which actually dominates is uncertain.

3.4   Methods and Experiment Design

To measure the likelihood of outcomes from Figure 3.4 we simulate competitive dynamics of the SI_1SI_2S model outlined in 3.1.1 over the CBMN model from Section 3.2. Each simulation for a given parameter set is composed of n independent trials ran in parallel; seeds are reset for each trial, providing reproducible random numbers which helps to isolate the effects of each experiment. Additionally, separate networks are generated for each trial, reducing the effects of chance topological characteristics that may create a fortuitous situation for one process over the other. Each r.v. S_1 and S_2 takes on the value 1 given the event that the corresponding process is still present in the population at the end of a single trial. From there we can calculate the conditional probabilities of survival and compare the resulting coexistence region to the one determined by marginal distributions.

In addition to measuring survival probability as a function of topological parameters, we also measure the average degree correlation between layers of each network. Degree correlation, ρ, is calculated as defined in[16]:

$$\rho(\mathcal{G}) = \frac{\sum_{i}^{N}(d_{E_1,i} - \bar{d}_{E_1})(d_{E_2,i} - \bar{d}_{E_2})}{\sqrt{\sum_{i}^{N}(d_{E_1,i} - \bar{d}_{E_1})^2}\sqrt{\sum_{i}^{N}(d_{E_2,i} - \bar{d}_{E_2})^2}} \tag{3.10}$$

Every work to date that models competitive processes on a multilayer networks has noted the importance of correlation between each layer as an important determining factor for coexistence[8;13;14;16;17;19]. We measure layer correlation in order to place current findings into the context of past results.

Since we are only interested examining the effect of competition between processes on the outcome of simulations, spreading and topological parameters are specified so to make sure

that processes are not effect by insufficient spreading and topological characteristics. What this means is that spreading strengths and topological parameters are tuned such that both processes trivially survive in the extreme case of complete isolation between communities. The constant edge probability threshold for communities, p, we set as a multiple of the theoretical threshold for a large connected component in Erydős-Róyni networks[22], $p = 2\frac{log(N)}{N}$. This ensures communities are sufficiently connected to sustain a process in the first place. For the same reason, we artificially introduce each process randomly into $\frac{1}{5}$ of their home community. Networks are composed of 50 nodes, $N = 50$, and simulations are sufficiently long to arrive at steady state solutions, we find a value of $T = 2048s$ is well suited. Recovery rates are set to unity, $\delta_1 = \delta_2 = 1$, which trivially makes processes infectivities equal to the transmission probability: $\beta_2 = \tau_1$ and $\beta_2 = \tau_2$. The following sections outline conditions specific to each experiment.

3.4.1 The Effect of Home Community Bias

We vary the extent to which each home community is biased in support of its respective process by the parameter ϵ. As defined in equation 3.3, ϵ is a term that multiplies the constant threshold, p, for each home community. In these simulations, the threshold for interconnections between communities, p_c, is set to 2%; this value was arrived at by empirical observation. Results from the following experiment additionally suggest that a threshold up to 5% is sufficient for coexistence. The range over which ϵ varies is logarithmically distributed over the interval $[10^{-2}, 10]$ and each value of ϵ is simulated 200 times.

At some point ϵ will be large enough to guarantee coexistence due to the fact that the relative difference between the connectivity of home communities and the rest of the network is sufficiently large. The number of connections within each home community increases to the point that the competing processes have no chance of competing outside of their home community.

3.4.2 The Effect of Community Distinction

In addition to home community bias, we also vary the connections between each community. We set $\epsilon = 2$, a value that will enable sufficient community structure for coexistence, by varying p_c over the interval $[10^{-3}, 1]$ we once again are looking at the onset of coexistence and measuring marginal and conditional probabilities of survival. Similar to the previous section, we expect at some point the competing processes will undergo a transition between complete dominance and coexistence.

3.4.3 Unequal Competitors

The topological experiments outlined in Section 3.4.1 & 3.4.2 assume equal strength processes, any advantage that leads to the extinction of a process purely results from topological advantage. The results of both experiments are used to identify values for ϵ and p_c which we use in simulations where the strengths of processes are varied. As can be seen in the top two graphs of Figure 3.5, which show survival probabilities as a function of topological parameters, there exists a range of parameters for ϵ and p_c between the points where marginal and conditional are maximally different (at the point where conditional probabilities become non-zero) and where they converge. We use the mid-point of this interval, $\epsilon = 1.75$ and $p_c = .05$, as parameters for the CBMN model.

As stated previously, recovery rates are held constant at one, thus the strength of each virus is varied by the infection probability. Both τ_1 and τ_2 are varied over the interval $[0, .7]$ which is a sufficiently long range to observe all regimes of competitive behavior.

3.5 Results & Discussions

3.5.1 Home Bias & Community Distinction

The first experiment conducted is measuring the survival probability of processes by varying the connectivity within each community via the parameter ϵ. Results for this experiment can be seen on the left side of Figure 3.5. The top graph shows both marginal and conditional probabilities of each process surviving, marginal probabilities reach a steady state even for very low values of ϵ while conditional probabilities go to zero at $\epsilon = 1$. The base threshold for communities, p, defined in Section 3.2, is fairly large without the additional $1 + \epsilon$ term and produces fairly well connected communities. Thus the value of ϵ for which probabilities converge is somewhat "extreme".

The middle left graph which is a snapshot of the final state of simulation trials, simply referred to as a *final state matrix*. The x-axis is the network model parameter that we are changing and each unit on the y-axis is a specific trial execution thread. Each pixel represents the outcome of a single trial for a specific parameter value. Note that by using a set of reproducible random numbers for each trial, there is context provided between horizontal results. The difference between marginal and conditional coexistence is due to the two processes "trading off" between dominating the other.

The bottom left graph shows layer correlations — defined in equation 3.10 — averaged over all simulation trials, as might be expected, we observe a strong correspondence between the convergence of probabilities and the steep decline of layer correlations.
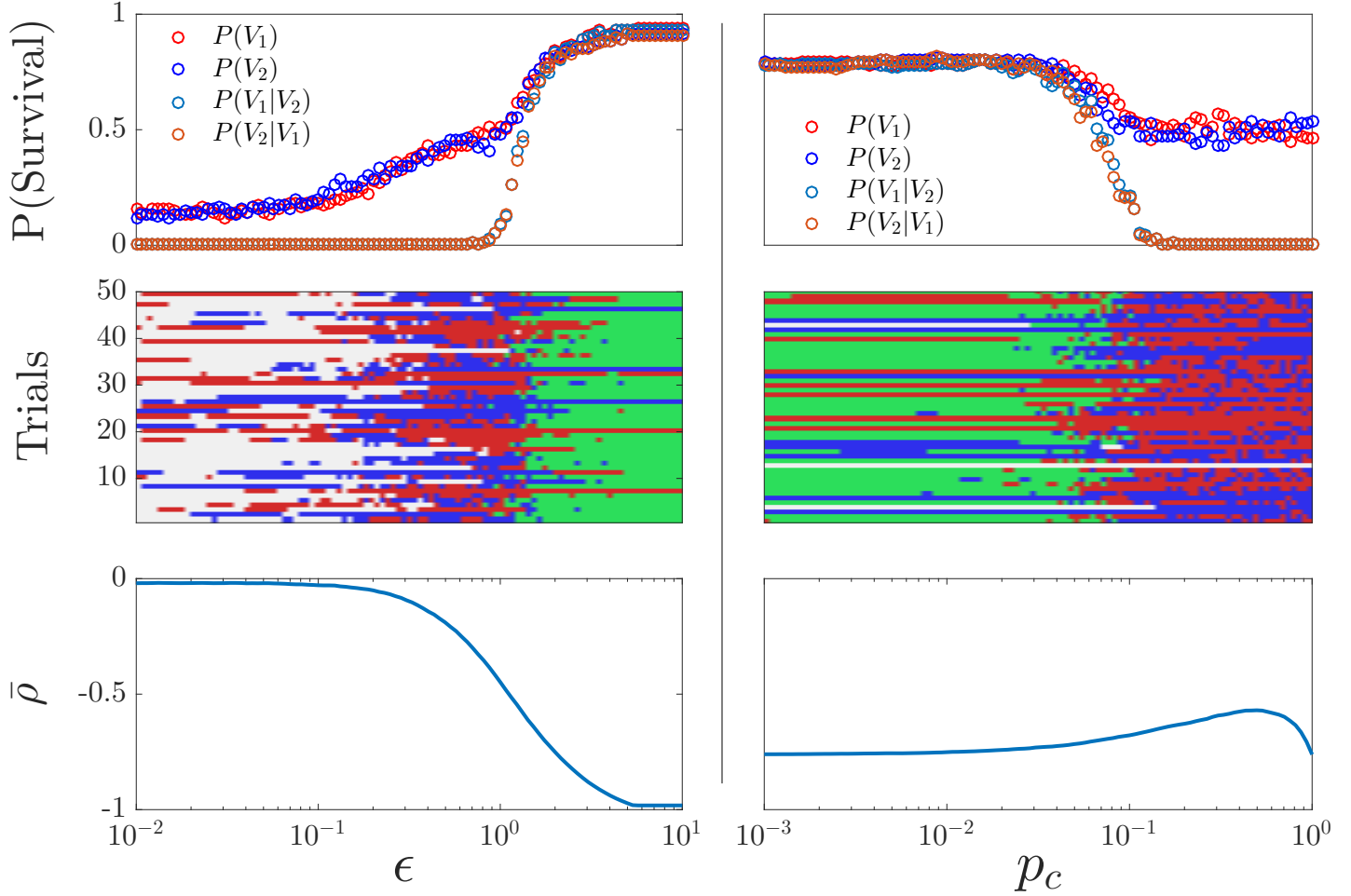
Figure 3.5: *Results on the left correspond to ϵ, home community bias and on the right, p_c, community distinction. (Top) Marginal and conditional probabilities of survival. The conditions for which they converge for ϵ are relatively tenuous, communities are already highly connected. (Middle) Final state matrix showing outcomes for a subset of the total amount of trials. Red marks indicate a trial where only process 1 survives, blue when only process 2, and green when both survive. (Bottom) the average correlation between layers. For ϵ the steep drop from low (negative) correlation to apparently perfectly anti-correlated corresponds to the transitions of the top two graphs. The behavior of $\hat{\rho}$ vs p_c is not as distinct with respect to the transitions above it, possibly suggesting fragile threshold for "real" coexistence.*

In the second experiment community distinction is varied by the parameter p_c. Essentially it is a different way to tune the multilayer network's ability to sustain coexistence. Instead of increasing bias in home communities, the distinction between communities is altered by connecting random nodes between them. The specific mechanism controlling coexistence may be different but the results for p_c are qualitatively the same as changing community bias, which is that we observe a threshold between regimes of agreement between survival probabilities. The relationship between community distinction and average layer correlation, $\hat{\rho}$, is not as stark as community bias; most likely due to the formulation of the multilayer model itself, p_c affects total overlap to a lesser extent than ϵ. Divergence of survival probabilities corresponds to the period where correlation measurements are increasing.

Past studies have all agreed that correlation between node degrees in each layer is an important factor in the coexistence of processes. The present results have not only confirmed that but also provided insight into the reason behind why layer correlation is closely tied with coexistence, since it is a sort of measure of community distinction.

3.5.2 Unequal Competitors

We simulated competitive processes over a range of strengths, the results of which can be seen in Figures 3.6 & 3.7. Values for ϵ and p_c were chosen based off method outlined in Section 3.4.3. In Figure 3.6 we observe a plot of survival probabilities, marginal on top and conditional on the bottom. Survival probabilities for each process are nearly symmetric, though skewed in favor of process 1 (red). The next figure, 3.7 shows a heatmap with marginal probabilities of coexistence in yellow and conditional coexistence in green. Evidently that marginal predictions of coexistence differ from conditional the most for infectivities that are relatively close to the epidemic threshold (around $\tau = .2$).

3.5.3 Comparing Mean-Field with Exact Results

Many formulations of compartmental models utilize the mean-field assumption in order to make the resulting coupled differential equations analytically tractable. As an aside, we com-
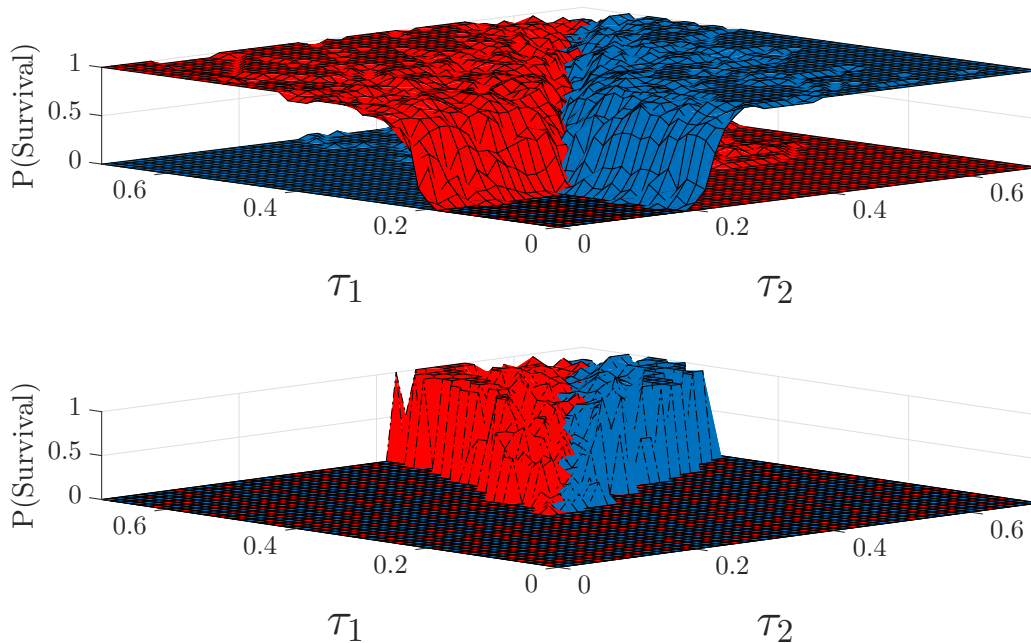
Figure 3.6: *3D Plot of competing processes for marginal and conditional probabilities. Red corresponds to process 1 and blue to process 2. On top are marginal probabilities, conditional are on bottom*

pare marginal survival probability with the coexistence thresholds predicted by mean-field theory [16]. From Figure 3.8 we observe a clear correspondence between theoretical predictions from mean-field approximations and marginal measurements. This demonstrates that the specific approximation technique does not account for the discrepancies we have presented; further underscoring the fact that the issue lies with relying on marginals.
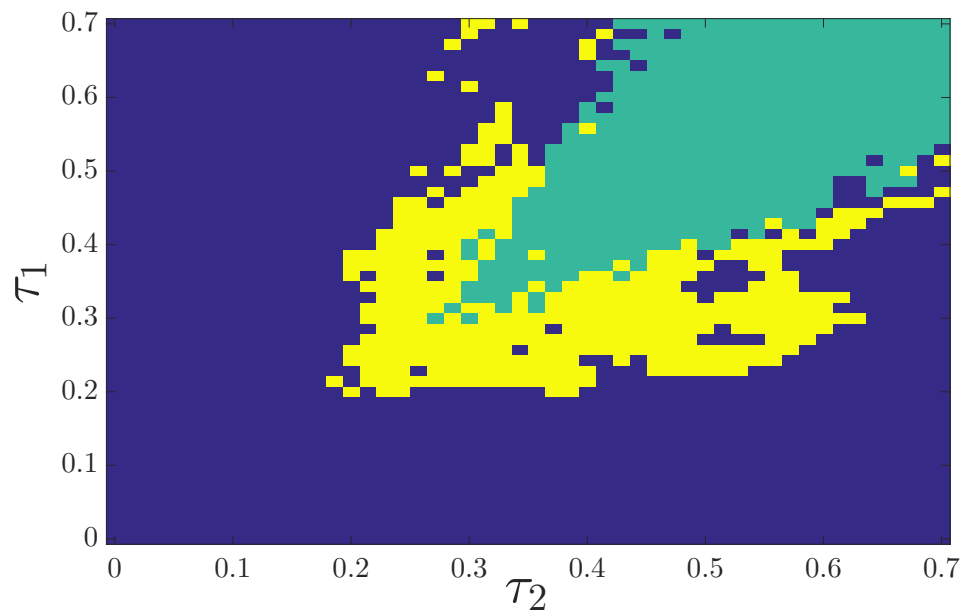
Figure 3.7: *Heatmap comparison of marginal & conditional coexistence probabilities. Yellow represents areas where only marginal probabilities are positive (for both processes), green where marginal and conditional probabilities are non-zero.*
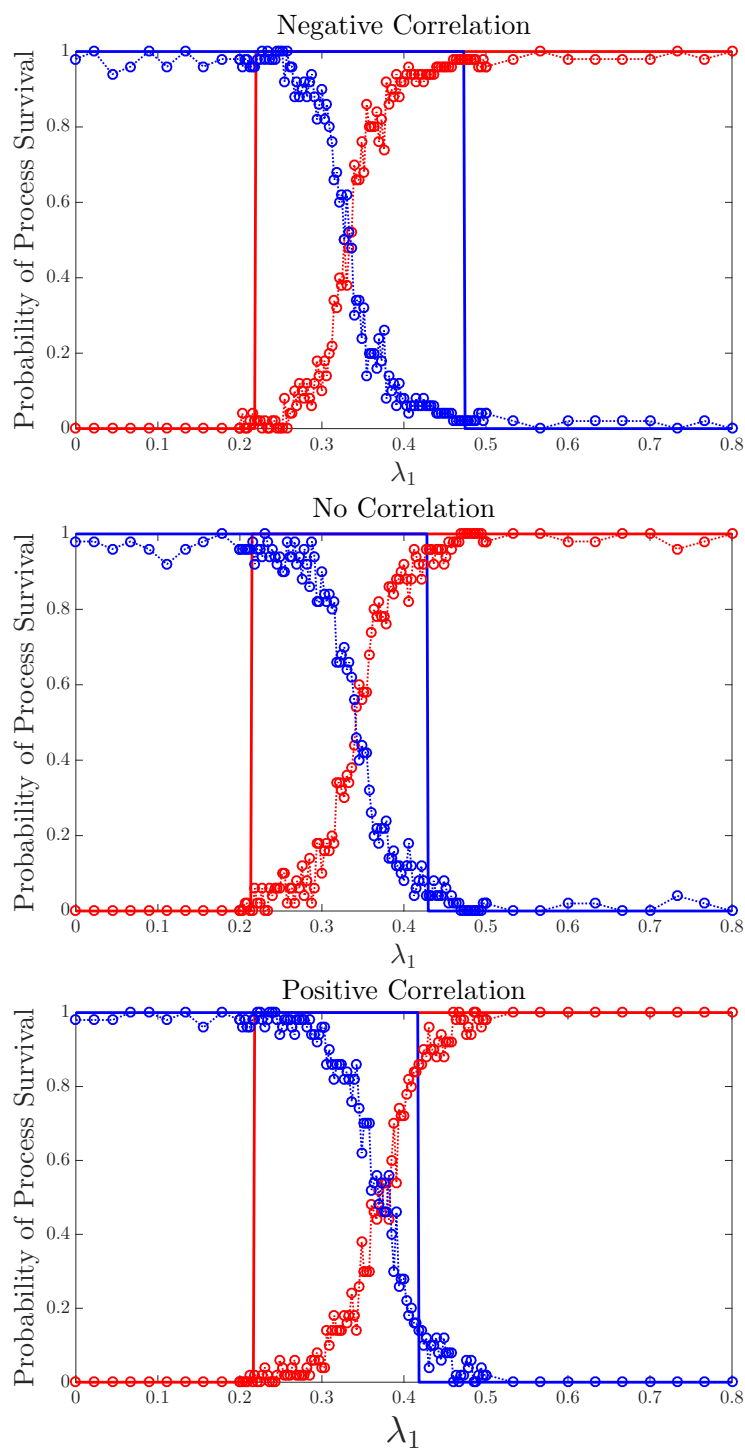
Figure 3.8: *Comparison of mean-field approximations from Sahneh et al for process 1 (red) and process 2 (blue).[16] (solid lines) and the actual solutions via stochastic simulations (denoted by marks). Mean-field approximations for marginal probabilities reasonably predict transition thresholds*

Chapter 4

Interacting Processes on Dynamic Networks

In addition to the investigations of coexistence outlined in the preceding chapter, work on a different scenario for interacting processes was also completed and is presented here. We perform numerical investigations into the behavior of interacting awareness and infectious processes over a dynamic contact network. Using a two layer network we define two separate families of contacts for each node, "normal" contacts which a node is initially in contact with, and a set of contacts which the node may "switch" to in the presence of an infection. The "switch" itself is a mechanism by which nodes implement adaptive behavior, thus we use the term adaptive contact network.

In a soon to be published paper this problem is fully explored, my contribution to the article were the numerical investigations of theoretical predictions. Thus in this chapter I will include only as much of the article as background that is needed to understand the context of the present authors contributions. We start by defining the dynamic epidemic process that will take place on top of the switching contact network which in turn motivates the multilayer adaptive contact network.

4.1 AC-SAIS

The *Adaptive Contact - Susceptible Aware Infected Suscetible* model is an extension of the $SAIS$ model which investigates the dynamics of interactions between an infection process and an awareness (of the infection) process that reduces the infection transition probability[23]. The key difference between the original $SAIS$ model and the current one, is that the awareness state does not inherently weaken the strength of the infection process. Instead it induces a topological change, which does not inherently aid or inhibit the infection, we find some interesting implications for the behavior of the epidemic threshold as a function of the alerting rate.
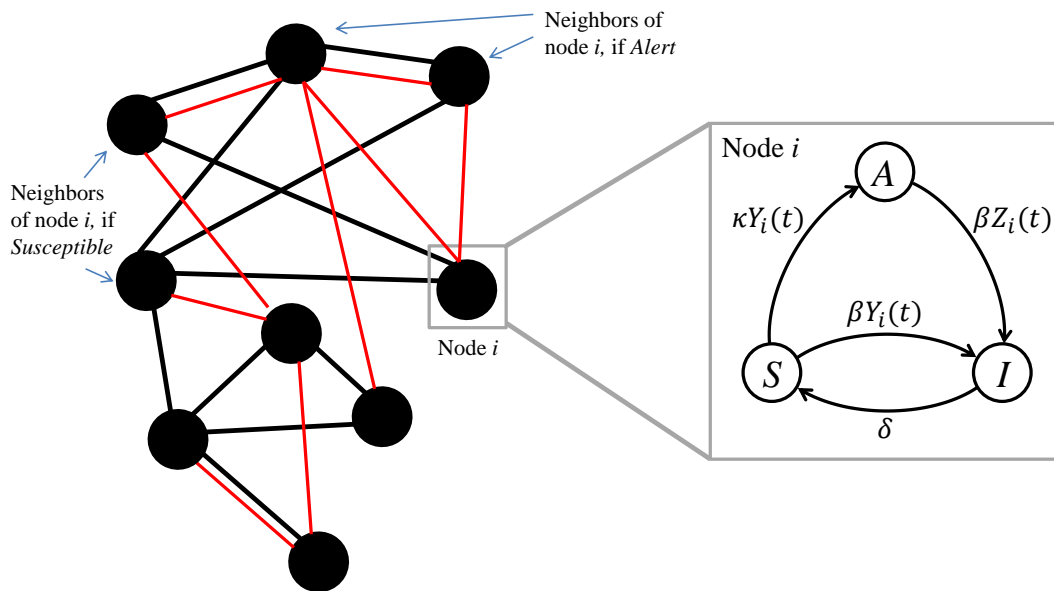
Figure 4.1: *Diagram of $AC-SAIS$ model and an illustration of an example multilayer network.*

As in the classic SIS model, we define a transmission probability, β, and recovery rate, δ. Additionally consider κ, the probability of a node transitioning to the *aware* state given infected neighbors. The state transition diagram can be seen in Figure 4.1. The following

differential equations are the mean-field approximate descriptions of the $AC-SAIS$ model:

$$\dot{p}_i = -\delta p_i + \beta(1 - q_i - p_i)\sum w_{ij}^S p_j + \beta q_i \sum w_{ij}^A p_j,$$

$$\dot{q}_i = \kappa(1 - q_i - p_i)\sum w_{ij}^S p_j - \beta q_i \sum w_{ij}^A p_j, \tag{4.1}$$

Where $\dot{p}_i$ is the marginal evolution of the infected state and $\dot{q}_i$ is the awareness.

From these the equations solutions for the epidemic threshold can be obtained:

$$\tau_c(\bar{\kappa}) = \frac{1}{\lambda_1(W_S)}(1 + \bar{\kappa}(\Psi(W_S, W_A) - 1)) + o(\bar{\kappa}),$$

$$\tau_c(\bar{\kappa}) = \frac{1}{\lambda_1(W_A)}(1 + \bar{\kappa}^{-1}(\Psi(W_A, W_S) - 1)) + o(\bar{\kappa}^{-1}) \tag{4.2}$$

where $\bar{\kappa}$ is a normalized alerting rate, W_S & W_A are adjacency matrices for each layer. $\Psi(A, B)$ is defined as:

$$\Psi(A, B) \triangleq \sum_{i=1}^{N} u_i v_i \frac{\sum_{j=1}^{N} a_{ij} v_j}{\sum_{j=1}^{N} b_{ij} v_j}, \tag{4.3}$$

$\boldsymbol{v}_A = [v_1, ..., v_N]^T$ and $\boldsymbol{u}_A = [u_1, ..., u_N]^T$ are the right and left dominant eigenvectors of A corresponding to $\lambda_1(A)$ with $\boldsymbol{v}_A^T \boldsymbol{u}_A = 1$. Figure 4.2 shows three different regimes of solutions to equations 4.2 which occur due to the configuration of node degrees and eigenvectors.

4.2 Adaptive Contact Network Model

For a network of size N, each node has one of two contact sets active at a given time, meaning the complete ensemble of possible states (with regards to topology) the network may be in is of size 2^N. One approach to modeling epidemic processes on this network would be to define a Markov process describing transitions between each of the 2^N possible networks; clearly, a cumbersome task that does not scale well. It is the novel contribution of the soon to be published article, of which this work is a small part, to avoid this obstacle entirely by defining an equivalent 2-layer network representation which incorporates the full 2^N state space.
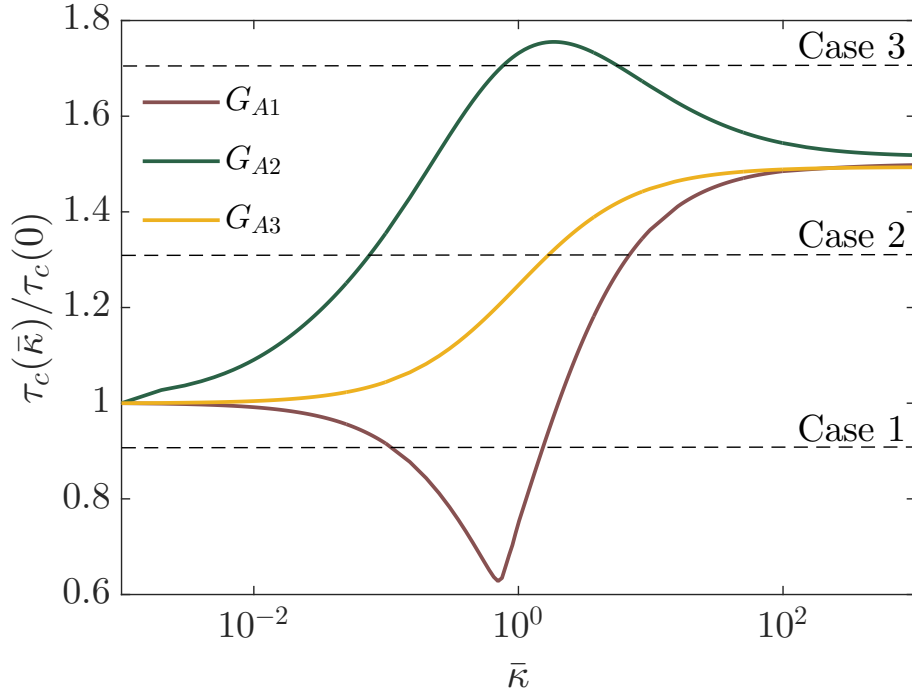
Figure 4.2: *Normalized epidemic threshold $\tau_c(\bar{\kappa})/\tau_c(0)$ as a function of normalized alerting rate $\bar{\kappa}$, showing all three dependency scenarios.*

4.3 Experimental Setup

We use the well known "Football" network from [24] with $N = 115$ nodes and $|E_S| = 615$ edges, and spectral radius 10.8. Given G_S, the unaltered football we synthesize three alert contact edges E_{A1}, E_{A2}, and E_{A3} such that the following conditions are met:

1. The spectral radii of G_{Ai} graphs are all equal to $\frac{2}{3}$ of the spectral radius of G_S, i.e. $\lambda_1(W_{Ai}) = \frac{2}{3}\lambda_1(W_S)$. Guaranteeing that the alert contact layers are more robust to epidemic spreading compared to the default contacts layer.

2. For G_{A1}, $\Psi(W_S, W_{A1}) < 1$. From Equation 4.2, we predict that for small values of $\bar{\kappa}$, the epidemic threshold decreases below the threshold if no contact adaptation was in place at all.

3. For G_{A2}, $\Psi(W_{A2}, W_S) > 1$. From Equation 4.2, it is also possible to for the epidemic threshold of the multilayer network to be greater than its constituent layers. In this

configuration, the characteristics are such that an enhanced robustness is created syn-ergistically.

4. Graph G_{A3} is made by decreasing the link weights from G_S, which we expect to see a monotonic increase in the epidemic threshold as the contact adaptation rate increases.

All three alert layers have the same spectral radius with respect to G_S i.e. $\lambda_1(W_S)/\lambda_1(W_{Ai}) = 1.5$. Therefore, in all of them the threshold value $\tau_c(\bar{\kappa})$ starts from $\tau_c(0) = 1/\lambda_1(W_S)$ and converges to $\tau_c(\infty) = 1.5\tau_c(0)$. Graph G_{A1} is synthesized such that $\Psi(W_S, W_{A1}) < 1$. From the red curve we can observe that $\tau_c(\bar{\kappa})$ decreases for small $\bar{\kappa}$ values after which it increases. Graph G_{A2} is synthesized such that $\Psi(W_S, W_{A2}) > 1$. In this case the green curve $\tau_c(\bar{\kappa})$ is maximal around $\bar{\kappa} \approx 2$. The topology of graph G_{A3} is G_S with reduced weights and is represented by the yellow epidemic threshold curve which increases monotonically by $\bar{\kappa}$.

In order to synthesize G_{A1} and G_{A2}, we performed a greedy search to obtain desired values of Ψ functions. For each alert contact graph, G_{Ai}, and subsequent multilayer network representation, $\mathcal{G}_i = (V, E_S, E_{Ai})$, we examine spreading behavior at three effective infection rates seen in Fig. 4.2 (dotted lines). Steady-state solutions to the mean-field AC-SAIS Equations 4.1 are calculated for $10^{-3} \leq \bar{\kappa} \leq 10^2$ and fraction of population infected $\bar{p} = \frac{1}{N}\sum_{i=1}^{N} p_i$—as the indicator of severity of an epidemic—is plotted as a function of the alerting rate.

4.4 Results

4.4.1 Adaptation gone wrong

In the top plot of Figure 4.3, we can see that for most alert values, κ, there is no outbreak, as one would expect since the effective infection rate is below the epidemic threshold for each layer. However, for $.03 \leq \bar{\kappa} \leq .6$ an epidemic is sustained due entirely to inter-layer dynamics that create conditions where an epidemic is more effectively carried throughout the population. Indicating that persons who alter who they come into contact with, although in

an effort to avoid becoming infected, may in fact unintentionally contribute to the opposite outcome. For case 2, with $\tau_c(0) < \tau < \tau_c(\infty)$, we observe two regimes of behavior: for lower alerting rates, where the effective infection rate is below the epidemic threshold $\tau_c(\bar{\kappa})$, an infection is sustained. For higher alerting rates the reverse is true since the critical threshold goes above τ. In case 3, effective infection rate is set above the critical threshold for all values of $\bar{\kappa}$, i.e., $\tau_c(\bar{\kappa}) < \tau$. Therefore, persistent infections are observed regardless of contact adaptation rate.
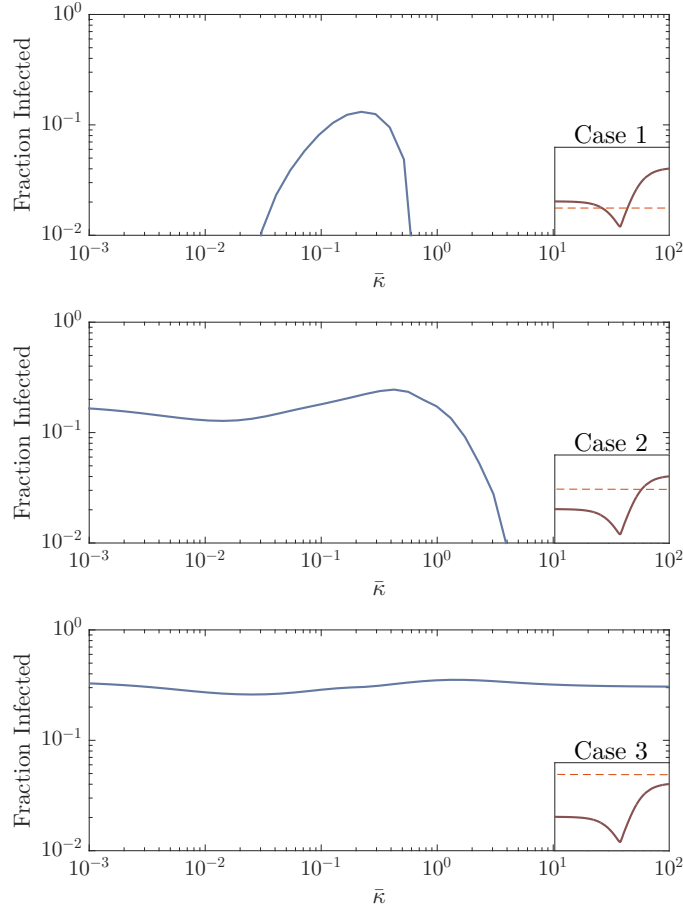
Figure 4.3: *The effect of alerting rate on infection size for the undershooting scenario.*
Case 1 *Despite setting the effective infection rate below that of the extreme cases, i.e.,*
$\tau < \tau_c(0) < \tau_c(\infty)$, *an epidemic outbreak is still observed for small alerting rates because* τ
is larger than the minimum of $\tau_c(\bar{\kappa})$.
case 2 *Effective infection rate lies in between the two extreme values, i.e.,* $\tau_c(0) < \tau < \tau_c(\infty)$.
There is a slight increase in infected individuals around the minimum of the threshold curve
after which the infection size drops to 0 *due to the increase in the critical threshold.*
case 3 *The effective infection rate is set above the critical threshold for all* $\bar{\kappa}$, *i.e.,* $\tau_c(\bar{\kappa}) < \tau$.
Therefore an infection is sustained regardless of the alerting rate.

4.4.2 Enhanced robustness

For the same set of computations on graph $\mathcal{G}_2$. Case 1 yields trivially zero infection size. For case 2, shown in the top plot of Fig. 4.4, we observe that increasing alerting rate beyond a certain value successfully suppresses the infection spreading. **Case 3** provides an interesting observation in that the critical threshold raises even larger than the alert contacts layer, indicating that a moderate rate of contact adaptation is indeed better than fast rates in enhancing the robustness of the network. Therefore, for $\bar{\kappa}$ values around 1, the critical threshold increases such that no infection is sustained. While for a larger values an outbreak occurs, and the infection size increases as contact adaptation rate is increases.
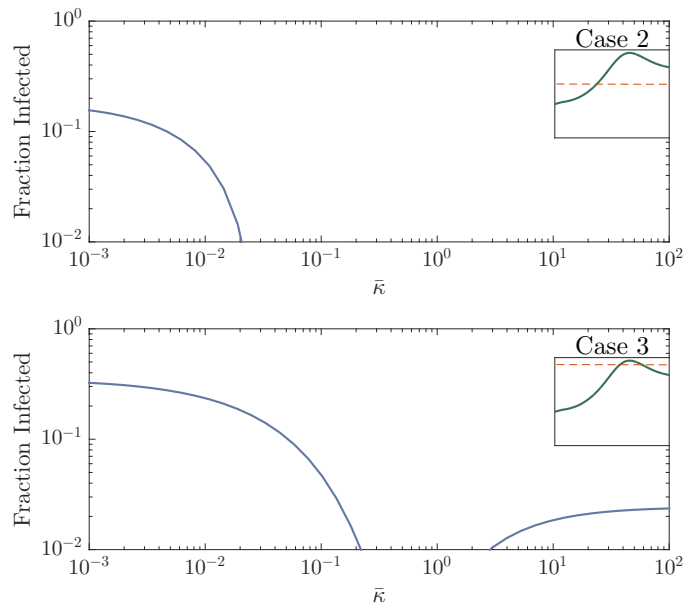
Figure 4.4: *The effect of alerting rate on infection size for the overshooting scenario.*
case 1 *This case is omitted since the infection size would be* 0 *regardless of the alerting rate*
case 2 *The behavior is similar to case 2 with* G_{A1} *(middle graph in Fig. 4.3) though the transition to a more robust threshold (due to increased alert state occupants) occurs at a smaller alerting rate.*
case 3 *One of the more interesting scenarios is when the effective infection rate is larger than the extreme values, i.e.,* $\tau_c(0) < \tau_c(\infty) < \tau$ *yet is less than the maximum of the threshold curve* $\tau_c(\bar{\kappa})$*. A non-zero infection size is observed for small alerting rates, eventually* $\bar{\kappa}$ *raises above* τ *so that an epidemic cannot be sustained. As the threshold converges towards* $\tau_c(\infty)$*, an epidemic can once again persist, and the infection size even increases by the contact adaptation rate.*

4.4.3 Monotonic Dependency

The monotonically increasing threshold curve of $\mathcal{G}_3$ in Fig. 4.2 is the result one would intuitively expect (or at least hope for) from adaptive contact behavior. Meaning, that when considering nodes can "switch" to a neighborhood constituting a more robust network, the intuitive, expected effect on the overall robustness of the network would be to increase monotonically with the alerting rate. As the previous two sections have shown, this is not always the case. Indeed, we observed non-monotone dependency of the epidemic threshold in most of our experiment trials. However, we can see that in some cases, case 2 for example, the epidemic response for the three network configurations are generally the same. They differ only so far as where the transition from sustaining an infection to not occurs.
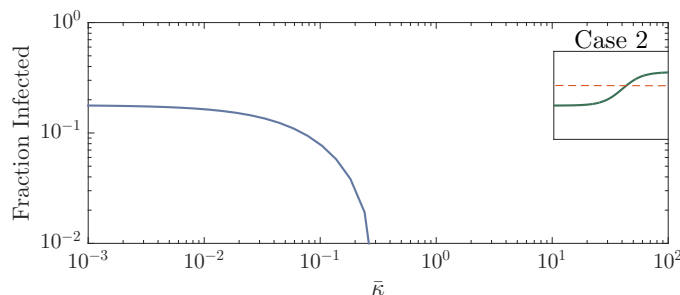
Figure 4.5: *The effect of alerting rate on infection size for the monotonically increasing threshold curve.*
case 2 *Similar to Sections 4.4.1 and 4.4.2, case 2 shows a transition between low and high alerting rates where epidemic outbreaks occur for the former and not the latter*
Cases 1 and 3 are omitted for trivial behavior.

Chapter 5

Final Words

The work presently submitted in fulfillment of the Master's thesis requirement has showcased the author's research into the dynamics of interacting processes. With respect to the coexistence of interacting processes, a case has been presented against the effectiveness of marginal population dynamics to accurately characterize coexistence. Support for this conclusion is based on the experimental results of processes competing over a community-based multi-layer network model. Previous investigations have indicated that sufficiently anti-correlated contact networks are crucial to coexistence. The CBMN model exploits this to generate topologies which trivially support co-survival of processes by way of isolation. By measuring the survival outcome distribution for each process we demonstrated that though marginal descriptions of survival correspond well with predictions of previous studies, they were not reliable indicators of true coexistence i.e. where *both* processes are present at the end of the same trial.

At the very least these results indicate the need for further investigation and may in the future give pause when choosing to model interacting processes. Take as an example, the LotkaVolterra equations[25], which model dynamics of predator-prey interactions by defining two differential equations describing the populations of each. Coexistence among the two species is determined by positive solutions to the dynamical equations, so an interesting and possibly important question to ask would be if situations such as the LotkaVolterra equations

are perhaps flawed in the same respect as the situations presented here.

Bibliography

[1] Faryad Darabi Sahneh, Caterina Scoglio, and Piet Van Mieghem. Generalized epidemic mean-field model for spreading processes over multilayer complex networks. *IEEE/ACM Transactions on Networking*, 21(5):1609–1620, 2013.

[2] Xiang Wei, Shihua Chen, Xiaoqun Wu, Jianwen Feng, and Jun-an Lu. A unified framework of interplay between two spreading processes in multiplex networks. *EPL (Europhysics Letters)*, 114(2):26006, 2016.

[3] Faryad Darabi Sahneh. *Spreading processes over multilayer and interconnected networks*. PhD thesis, Kansas State University, 2014.

[4] Manlio De Domenico, Clara Granell, Mason A Porter, and Alex Arenas. The physics of spreading processes in multilayer networks. *Nature Physics*, 2016.

[5] Romualdo Pastor-Satorras, Claudio Castellano, Piet Van Mieghem, and Alessandro Vespignani. Epidemic processes in complex networks. *Reviews of modern physics*, 87 (3):925, 2015.

[6] Mostafa Salehi, Rajesh Sharma, Moreno Marzolla, Matteo Magnani, Payam Siyari, and Danilo Montesi. Spreading processes in multilayer networks. *IEEE Transactions on Network Science and Engineering*, 2(2):65–83, 2015.

[7] Faryad Darabi Sahneh, Aram Vajdi, Heman Shakeri, Futing Fan, and Caterina Scoglio. Gemfsim: A stochastic simulator for the generalized epidemic modeling framework. *arXiv preprint arXiv:1604.02175*, 2016.

[8] M. E. J. Newman. Threshold effects for two pathogens spreading on a network. *Phys. Rev. Lett.*, 95:108701, Sep 2005. doi: 10.1103/PhysRevLett.95.108701. URL http://link.aps.org/doi/10.1103/PhysRevLett.95.108701.

[9] B Aditya Prakash, Alex Beutel, Roni Rosenfeld, and Christos Faloutsos. Winner takes all: competing viruses or ideas on fair-play networks. In *Proceedings of the 21st international conference on World Wide Web*, pages 1037–1046. ACM, 2012.

[10] Ruud van de Bovenkamp, Fernando Kuipers, and Piet Van Mieghem. Domination-time dynamics in susceptible-infected-susceptible virus competition on networks. *Physical Review E*, 89(4):042818, 2014.

[11] Alex Beutel, B Aditya Prakash, Roni Rosenfeld, and Christos Faloutsos. Interacting viruses in networks: can both survive? In *Proceedings of the 18th ACM SIGKDD international conference on Knowledge discovery and data mining*, pages 426–434. ACM, 2012.

[12] Garrett Hardin et al. The competitive exclusion principle. *science*, 131(3409):1292–1297, 1960.

[13] Sebastian Funk and Vincent AA Jansen. Interacting epidemics on overlay networks. *Physical Review E*, 81(3):036118, 2010.

[14] Vincent Marceau, Pierre-André Noël, Laurent Hébert-Dufresne, Antoine Allard, and Louis J Dubé. Modeling the dynamical interaction between epidemics on overlay networks. *Physical Review E*, 84(2):026105, 2011.

[15] Joaquín Sanz, Cheng-Yi Xia, Sandro Meloni, and Yamir Moreno. Dynamics of interacting diseases. *Physical Review X*, 4(4):041005, 2014.

[16] Faryad Darabi Sahneh and Caterina Scoglio. Competitive epidemic spreading over arbitrary multilayer networks. *Physical Review E*, 89(6):062817, 2014.

[17] Nicholas J Watkins, Cameron Nowzari, Victor M Preciado, and George J Pappas. Optimal resource allocation for competing epidemics over arbitrary networks. In *2015 American Control Conference (ACC)*, pages 1381–1386. IEEE, 2015.

[18] Clara Granell, Sergio Gómez, and Alex Arenas. Dynamical interplay between awareness and epidemic spreading in multiplex networks. *Physical review letters*, 111(12):128701, 2013.

[19] Xuetao Wei, Nicholas C Valler, B Aditya Prakash, Iulian Neamtiu, Michalis Faloutsos, and Christos Faloutsos. Competing memes propagation on networks: A network science perspective. *IEEE Journal on Selected Areas in Communications*, 31(6):1049–1060, 2013.

[20] Xiang Wei, Shihua Chen, Xiaoqun Wu, Di Ning, and Jun-an Lu. Cooperative spreading processes in multiplex networks. *Chaos: An Interdisciplinary Journal of Nonlinear Science*, 26(6):065311, 2016.

[21] Emmanuel Abbe, Afonso S Bandeira, and Georgina Hall. Exact recovery in the stochastic block model. *IEEE Transactions on Information Theory*, 62(1):471–487, 2016.

[22] Mark Newman. *Networks: an introduction.* Oxford university press, 2010.

[23] Faryad Darabi Sahneh, Fahmida N. Chowdhury, and Caterina M. Scoglio. On the existence of a threshold for preventive behavioral responses to suppress epidemic spreading. *Sci. Rep.*, 2, 2012.

[24] Michelle Girvan and Mark EJ Newman. Community structure in social and biological networks. *Proceedings of the national academy of sciences*, 99(12):7821–7826, 2002.

[25] Alan A Berryman. The orgins and evolution of predator-prey theory. *Ecology*, 73(5): 1530–1535, 1992.